forces acting on it: repulsion between one of the water H atoms and the Na cations, and hydrogen bonding of the other H atom to the O1 framework oxygens surrounding the structural channel. These rather weak bonding contacts allow a large freedom of motion of the water molecules about their equilibrium position (Boutin, Prask & Safford, 1965) so that the water has a clear zeolitic character, although a strict alternation of water molecules and Na cations along the channel makes hydration and dehydration processes in beryl rather difficult even under hydrothermal conditions (Wood & Nassau, 1968), since the alkali cations are effectively limiting the diffusion of the water molecules.

The observed geometry of the water molecules in site 2(*a*) may be interpreted as an ensemble of positions having a common direction of one O—H vector, and can partially explain why in alkali-rich beryls both type I and type II water molecules have been reported from spectroscopic measurements.

The SERC is acknowledged for neutron beam time at ISIS. The experiment was partially supported by a grant under the CNR-SERC agreement. General financial support was provided by Italian MURST (40 and 60% research funds). Anonymous referees supplied useful discussion and suggestions.

References

AINES, R. G. & ROSSMAN, G. R. (1984). *Am. Mineral.* **69**, 319–327.
ARTIOLI, G., RINALDI, R., STÅHL, K. & ZANAZZI, P. F. (1993). *Am. Mineral.* **78**, 762–768.
AURISICCHIO, C., FIORAVANTI, G., GRUBESSI, O. & ZANAZZI, P. F. (1988). *Am. Mineral.* **73**, 826–837.
BATS, J. W., FUESS, H. & ELERMAN, Y. (1986). *Acta Cryst.* B**42**, 552–557.
BOUTIN, H., PRASK, H. & SAFFORD, G. J. (1965). *J. Chem. Phys.* **42**, 1469–1470.
BROWN, G. E. & MILLS, B. A. (1986). *Am. Mineral.* **71**, 547–556.
CHIARI, G. & FERRARIS, G. (1982). *Acta Cryst.* B**38**, 2331–2341.
COPPENS, P. (1969). *Acta Cryst.* A**25**, 180–186.
COPPENS, P., DAM, J., HARKEMA, S., FEIL, D., FELD, R., LEHMANN, M. S., GODDARD, R., KRÜGER, C., HELLNER, E., JOHANSEN, H., LARSEN, F. K., KOETZLE, T. F., MCMULLAN, R. K., MASLEN, E. N. & STEVENS, E. D. (1984). *Acta Cryst.* A**40**, 184–195.
COPPENS, P., SABINE, T. M., DELAPLANE, R. G. & IBERS, J. A. (1969). *Acta Cryst.* B**25**, 2451–2458.
GIBBS, G. V., BRECK, D. W. & MEAGHER, E. P. (1968). *Lithos*, **1**, 275–285.
HAMILTON, W. C. (1969). *Acta Cryst.* A**25**, 194–206.
HAWTHORNE, F. C. & ČERNÝ, P. (1977). *Can. Mineral.* **15**, 414–421.
LARSON, A. C. & VON DREELE, R. B. (1994). *GSAS Generalized Structure Analysis System.* Document LAUR 86-748. Los Alamos National Laboratory.
NORTH, A. C. T., PHILLIPS, D. C. & MATHEWS, F. S. (1968). *Acta Cryst.* A**24**, 351–359.
REHM, H.-J. (1974). *Z. Naturforsch. Teil A*, **29**, 1558–1571.
SANDERS, I. S. & DOFF, D. H. (1991). *Mineral. Mag.* **55**, 167–172.
SHERRIFF, B. L., GRUNDY, H. D., HARTMAN, J. S., HAWTHORNE, F. C. & ČERNÝ, P. (1991). *Can. Mineral.* **29**, 271–285.
VORMA, A., SAHAMA, T. G. & HAAPALA, I. (1965). *C. R. Soc. Geol. Fin.* **37**, 119–129.
WICKERSHEIM, K. A. & BUCHANAN, R. A. (1959). *Am. Mineral.* **44**, 440–445.
WICKERSHEIM, K. A. & BUCHANAN, R. A. (1965). *J. Chem. Phys.* **42**, 1468–1469.
WOOD, D. L. & NASSAU, K. (1967). *J. Chem. Phys.* **47**, 2220–2228.
WOOD, D. L. & NASSAU, K. (1968). *Am. Mineral.* **53**, 777–800.

Acta Cryst. (1995). B**51**, 737–745

Site Preference of Cations and Structural Variation in $Y_3Fe_{5-x}Ga_xO_{12}$ ($0 \le x \le 5$) Solid Solutions with Garnet Structure

BY AKIHIKO NAKATSUKA,* AKIRA YOSHIASA† AND SETSUO TAKENO

Faculty of Science, Hiroshima University, Higashi-Hiroshima, Hiroshima 724, *Japan*

(*Received* 25 *November* 1993; *accepted* 19 *December* 1994)

Abstract

The crystal structures of $Y_3Fe_{5-x}Ga_xO_{12}$ ($0 \le x \le 5$) solid solutions ($x = 0.0$, 1.0, 1.6, 2.0, 2.5, 3.0, 3.6, 3.8, 4.6 and 5.0) with garnet structure were refined by single-crystal X-ray diffraction analyses. Site preferences of cations in the crystal structure were examined in detail. The smaller Ga^{3+} ion occupies only the four-coordinated site in the composition range $x = 0.0$–1.6 (region I), whereas the larger Fe^{3+} ion occupies only the six-coordinated site from $x = 5.0$ to 3.8 (region III). Both cations occupy these two sites from $x = 1.6$ to 3.8 (region II). The tendency for site preference of cations changes near $x = 1.6$ and 3.8. When Ga^{3+} and Fe^{3+} occupy only the four- (region I) and six-coordinated sites (region III), respectively, the enhancement of the cation–cation interaction can be considered as a result of the geometric restriction due to the variation of cation size. The change in tendency for cation site preference is most probably caused by the increased cation–cation interaction. Crystal data: cubic, $Ia\bar{3}d$, $Z = 8$, Mo $K\alpha$, $\lambda = 0.71069$ Å; at $x = 0.0$: $a_0 = 12.375(1)$ Å,

* Present address: The Institute of Scientific and Industrial Research, Osaka University, Ibaraki, Osaka 567, Japan.
† Present address: Faculty of Science, Osaka University, Toyonaka, Osaka 560, Japan.

$V = 1895.3(3)$ Å^3, $D_x = 5.17$ Mg m^{-3}, $M_r = 737.938$, $\mu = 26.42$ mm^{-1}, $F(000) = 2744$, $R = 0.020$ for 144 reflections; at $x = 1.0$: $a_0 = 12.360(1)$ Å, $V = 1888.2(4)$ Å^3, $D_x = 5.29$ Mg m^{-3}, $M_r = 751.811$, $\mu = 27.95$ mm^{-1}, $F(000) = 2784$, $R = 0.019$ for 131 reflections; at $x = 1.6$: $a_0 = 12.351(1)$ Å, $V = 1883.9(3)$ Å^3, $D_x = 5.36$ Mg m^{-3}, $M_r = 760.135$, $\mu = 28.88$ mm^{-1}, $F(000) = 2808$, $R = 0.021$ for 110 reflections; at $x = 2.0$: $a_0 = 12.342(1)$ Å, $V = 1880.1(4)$ Å^3, $D_x = 5.41$ Mg m^{-3}, $M_r = 765.684$, $\mu = 29.51$ mm^{-1}, $F(000) = 2824$, $R = 0.018$ for 117 reflections; at $x = 2.5$: $a_0 = 12.333(1)$ Å, $V = 1875.8(3)$ Å^3, $D_x = 5.47$ Mg m^{-3}, $M_r = 772.621$, $\mu = 30.30$ mm^{-1}, $F(000) = 2844$, $R = 0.015$ for 111 reflections; at $x = 3.0$: $a_0 = 12.317(1)$ Å, $V = 1868.7(3)$ Å^3, $D_x = 5.54$ Mg m^{-3}, $M_r = 779.557$, $\mu = 31.14$ mm^{-1}, $F(000) = 2864$, $R = 0.017$ for 119 reflections; at $x = 3.6$: $a_0 = 12.312(2)$ Å, $V = 1866.2(5)$ Å^3, $D_x = 5.61$ Mg m^{-3}, $M_r = 787.881$, $\mu = 32.06$ mm^{-1}, $F(000) = 2888$, $R = 0.016$ for 168 reflections; at $x = 3.8$: $a_0 = 12.302(1)$ Å, $V = 1861.8(4)$ Å^3, $D_x = 5.64$ Mg m^{-3}, $M_r = 790.655$, $\mu = 32.42$ mm^{-1}, $F(000) = 2896$, $R = 0.020$ for 117 reflections; at $x = 4.6$: $a_0 = 12.289(1)$ Å, $V = 1856.1(3)$ Å^3, $D_x = 5.73$ Mg m^{-3}, $M_r = 801.754$, $\mu = 33.69$ mm^{-1}, $F(000) = 2928$, $R = 0.013$ for 103 reflections; at $x = 5.0$: $a_0 = 12.273(1)$ Å, $V = 1848.7(4)$ Å^3, $D_x = 5.80$ Mg m^{-3}, $M_r = 807.303$, $\mu = 34.45$ mm^{-1}, $F(000) = 2944$, $R = 0.021$ for 118 reflections.

Introduction

A number of artificial crystals with garnet structure have been investigated in the field of material sciences. Typical examples are $Y_3Al_5O_{12}$ and $Gd_3Ga_5O_{12}$ doped with Nd^{3+} as laser crystals and $Y_3Fe_5O_{12}$ (iron yttrium oxide/yttrium iron garnet, YIG) as ferrimagnetic crystals. The latter shows various interesting magnetic properties. YIG was first discovered by Bertaut & Forrat (1956) and further investigated by Geller & Gilleo (1957). The crystal structure of garnet was first determined by Menzer (1926). The structure belongs to the space group $Ia\bar{3}d$ with cations in special positions (24*c*, 16*a* and 24*d* sites) and oxygen anions in general positions (96*h* site). The structure has many shared edges between adjacent polyhedra. The tetrahedron and octahedron share edges with two and six triangular dodecahedra, respectively. The triangular dodecahedron shares edges with two tetrahedra, four octahedra and four other triangular dodecahedra, respectively. Tetrahedra and octahedra are linked by sharing all corners (Fig. 1). Substituted YIG materials ($Y_3M_{5-x}M'_xO_{12}$; M, M' = Al^{3+}, Fe^{3+}, Ga^{3+} *etc.*) have been investigated by several authors (e.g. Fischer, Hälg, Stoll & Segmüller, 1966; Marezio, Remeika & Dernier, 1968; Fischer, Hälg, Roggwiller & Czerlinsky, 1975). Fischer *et al.* (1966) studied the site preference of Ga^{3+} in $Y_3Fe_{5-x}Ga_xO_{12}$ solid solutions by means of powder X-ray and neutron diffraction methods. Marezio *et al.* (1968) studied the site preference of Ga^{3+} in $Y_3Al_{5-x}Ga_xO_{12}$ solid solutions by single-crystal X-ray diffraction methods. They pointed out that Ga^{3+} occupies the four-coordinated site preferentially. However, the relation between site preference of cations and the structural variation was left to be solved. Moreover, temperature factors for each site in the $Y_3Fe_{5-x}Ga_xO_{12}$ system have not yet been determined, even in research by Fischer *et al.* (1966), due to the strong correlation between temperature factors of the eight- and four-coordinated sites.

In this study, the structural variation of $Y_3Fe_{5-x}Ga_xO_{12}$ will be discussed based on the crystal structures obtained by determination of anisotropic temperature factors for each site, with special attention to the cation site preference.

Experimental

Specimen

Single crystals of $Y_3Fe_{5-x}Ga_xO_{12}$ used in this study were grown by means of the flux method using a PbF_2 flux. Special grade reagents (99.99%) of Y_2O_3, α-Fe_2O_3 and Ga_2O_3 were used as starting materials and mixed together in molar ratios Y_2O_3:α-Fe_2O_3:Ga_2O_3 = $3:(5-x):x$. The mixtures were placed in a 30 cm^3 platinum crucible and heated slowly to 1473 K and cooled at 5 K h^{-1} to 1023 K in atmospheric conditions. The temperature in the furnace was stable within ±1 K. Composition and homogeneity of the

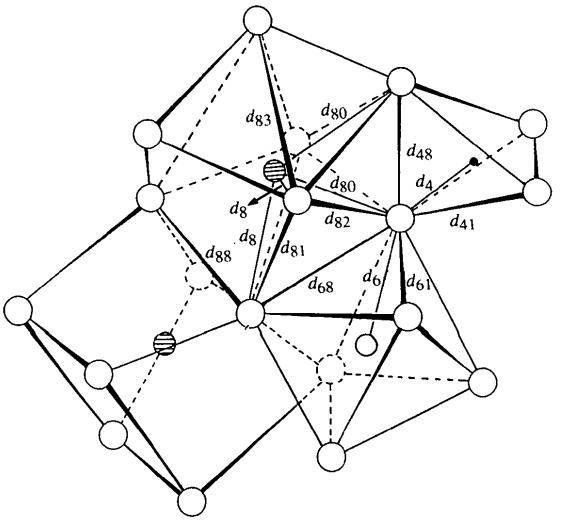

Fig. 1. Schematic coordination polyhedra of O atoms around Y, Fe and Ga atoms (after Novak & Gibbs, 1971). Large open circle (○), hatched circle (⊜), small open circle (○) and solid circle (●) represent O atoms, the eight-, six- and four-coordinated sites, respectively.

Table 1. *Crystal and refinement data*

Composition	$x = 0.0$	$x = 1.0$	$x = 1.6$	$x = 2.0$	$x = 2.5$	$x = 3.0$	$x = 3.6$	$x = 3.8$	$x = 4.6$	$x = 5.0$
a_0 (Å)	12.375 (1)	12.360 (1)	12.351 (1)	12.342 (1)	12.333 (1)	12.317 (1)	12.312 (2)	12.302 (1)	12.289 (1)	12.273 (1)
V (Å^3)	1895.3 (3)	1888.2 (4)	1883.9 (3)	1880.1 (4)	1875.8 (3)	1868.7 (3)	1866.2 (5)	1861.8 (4)	1856.1 (3)	1848.7 (4)
Space group	$Ia\bar{3}d$									
D_x (Mg m^{-3})	5.17	5.29	5.36	5.41	5.47	5.54	5.61	5.64	5.73	5.80
$F(000)$	2744	2784	2808	2824	2844	2864	2888	2896	2928	2944
Radiation used	Mo $K\alpha$									
Monochromator	graphite									
Crystal size (diam., mm)	0.130	0.150	0.160	0.090	0.095	0.130	0.135	0.190	0.115	0.220
μ (mm^{-1})	26.42	27.95	28.88	29.51	30.30	31.14	32.06	32.42	33.69	34.45
μr	1.72	2.10	2.31	1.33	1.44	2.02	2.16	3.08	1.94	3.79
Diffractometer	Rigaku AFC-5FOS									
Scan type	ω–2θ									
2θ range (°)	2–80	2–80	2–70	2–80	2–80	2–80	2–100	2–80	2–80	2–80
No. of measured reflections	1567	1555	1029	1555	1453	1550	2532	1451	1451	1529
No. of observed reflections after averaging with $\|F_o\| > 3\sigma(\|F_o\|)$	144	131	110	117	111	119	168	117	103	118
R_{int}	2.2	2.0	1.9	2.0	2.0	2.0	2.0	2.1	1.9	1.6
R (%)	2.0	1.9	2.1	1.8	1.5	1.7	1.6	2.0	1.3	2.1
wR (%)	2.2	1.9	2.1	1.9	1.5	1.9	1.6	2.2	1.4	2.2
Weighting scheme	$1/\sigma^2(F_o)$									

obtained crystals were examined using a JEOL JCMA-733II electron microprobe analyzer. The result of chemical analyses ascertained homogeneity of the crystals, and little compositional deviation was recognized. The ten crystals of $x = 0.0(1)$, $1.0(1)$, $1.6(1)$, $2.0(1)$, $2.5(1)$, $3.0(1)$, $3.6(1)$, $3.8(1)$, $4.6(1)$ and $5.0(1)$ were obtained.

X-ray intensity measurements

For intensity measurements, each single crystal was ground into a spherical shape with 0.09–0.22 mm in diameter and placed on a fine glass fiber (Table 1). Prior to intensity measurements, systematic absences of reflections (*hkl* reflections are present only with $h + k + l = 2n$; $0kl$ only with $k, l = 2n$; hhl only with $2h + l = 4n$; $h00$ only with $h = 4n$) were examined by means of Weissenberg photographs at room temperature. All results were consistent with the space-group symmetry $Ia\bar{3}d$.

The intensity data and lattice constants were obtained using a four-circle diffractometer (Rigaku AFC-5FOS) with graphite-monochromatized Mo $K\alpha$ radiation ($\lambda = 0.71069$ Å, 50 kV, 150–200 mA) at room temperature. The lattice constants were refined and determined by the least-squares method using the 2θ values of 25 reflections in the range $45 \leq 2\theta \leq 47°$. Intensities of reflections in the range $2 \leq 2\theta \leq 70°$ for the specimen with the composition $x = 1.6$, $2 \leq 2\theta \leq 100°$ for the composition $x = 3.6$ and $2 \leq 2\theta \leq 80°$ for all others were measured in the ω–2θ scan mode (Table 1). Intensity data were corrected for Lorentz and polarization factors and for absorption as a sphere ($\mu r = 1.33$–3.79 for Mo $K\alpha$ radiation, see Table 1). For all specimens, 1029–2532 reflections were measured and 103–168 significant independent reflections with $|F_o| > 3\sigma(|F_o|)$ were observed after averaging equivalent reflections, which were used for the refinements (Table 1). Coincidence factors of the equivalent reflections (R_{int} in Table 1) were 1.6–2.2%, showing good agreement.

Refinements

For rare-earth and yttrium garnets, the existence of reflections forbidden in space group $Ia\bar{3}d$, *i.e.* {222} and {666} reflections, has been noted by several workers (*e.g.* Popma, Van Diepen & Robertson, 1974; Chenavas, Joubert, Marezio & Ferrand, 1978). On this point, Guillot, Le Gall & Leblanc (1990) indicated that these reflections were present by the effect of multiple scattering. The forbidden reflections could not be observed in our study. Moreover, from Weissenberg photographs and the degree of coincidence for equivalent reflections, it is considered that there is no possibility of lower symmetry. Consequently, the symmetry of $Ia\bar{3}d$ was assumed in the present study.

The structural refinements were carried out using the full-matrix least-squares program *RFINE*2 (Finger, 1969). The starting values for the positional parameters used in this study were those of the weighted average values given by Euler & Bruce (1965) for $Y_3Fe_5O_{12}$ and $Y_3Ga_5O_{12}$. The isotropic temperature factors given by Bonnet, Delapalme, Fuess & Thomas (1975) for $Y_3Fe_5O_{12}$ were used. Atomic scattering curves for neutral atoms and correction terms for anomalous dispersion were taken from *International Tables for X-ray Crystallography* (1974).

Considering the effective ionic radii (Shannon, 1976), Y^{3+} can only occupy the eight-coordinated site, and Fe^{3+} and Ga^{3+} both the six- and four-coordinated sites. The occupancy parameter, therefore, was fixed in the eight-coordinated site and constrained between the six- and the four-coordinated sites. Consequently, in each cycle of refinements only the occupancy parameter of Ga^{3+} in the six-coordinated site was varied. During the least-squares refinements, correction for the isotropic extinction effect

Table 2. *Refined positional parameters and equivalent isotropic temperature factors* (Å^2), *and refined occupancy parameters*

$$B_{eq} = (4/3)\sum_i \sum_j B_{ij} a_i^* a_j^* \mathbf{a}_i.\mathbf{a}_j.$$

Composition (x)		x	y	z	B_{eq}	Occupancy parameters Ga^{3+}	Fe^{3+}
0.0	24(*c*)*	0.125	0	1/4	0.37		
	16(*a*)	0	0	0	0.46	(0.00)	(1.00)
	24(*d*)	0.375	0	1/4	0.49	(0.00)	(1.00)
	96(*h*)	−0.0269 (4)	0.0570 (4)	0.1501 (4)	0.50		
1.0	24(*c*)*				0.31		
	16(*a*)				0.43	0.00 (2)	1.00
	24(*d*)				0.73	0.33	0.67
	96(*h*)	−0.0279 (4)	0.0566 (3)	0.1511 (4)	0.46		
1.6	24(*c*)*				0.32		
	16(*a*)				0.44	0.03 (3)	0.97
	24(*d*)				0.68	0.50	0.50
	96(*h*)	−0.0283 (5)	0.0564 (5)	0.1516 (5)	0.56		
2.0	24(*c*)*				0.30		
	16(*a*)				0.48	0.08 (3)	0.92
	24(*d*)				0.74	0.61	0.39
	96(*h*)	−0.0277 (4)	0.0563 (4)	0.1514 (4)	0.50		
2.5	24(*c*)*				0.28		
	16(*a*)				0.41	0.18 (2)	0.82
	24(*d*)				0.60	0.71	0.29
	96(*h*)	−0.0273 (4)	0.0563 (4)	0.1512 (4)	0.62		
3.0	24(*c*)*				0.31		
	16(*a*)				0.45	0.22 (3)	0.78
	24(*d*)				0.69	0.86	0.14
	96(*h*)	−0.0275 (4)	0.0564 (4)	0.1514 (4)	0.41		
3.6	24(*c*)*				0.38		
	16(*a*)				0.45	0.47 (2)	0.53
	24(*d*)				0.51	0.88	0.12
	96(*h*)	−0.0279 (3)	0.0558 (3)	0.1510 (3)	0.59		
3.8	24(*c*)*				0.20		
	16(*a*)				0.45	0.38 (4) (0.40)†	0.62 (0.60)†
	24(*d*)				0.76	1.01 (1.00)†	−0.01 (0.00)†
	96(*h*)	−0.0282 (5)	0.0550 (5)	0.1507 (6)	0.43		
4.6	24(*c*)*				0.23		
	16(*a*)				0.32	0.81 (2)	0.19
	24(*d*)				0.54	1.00	0.00
	96(*h*)	−0.0276 (4)	0.0551 (4)	0.1499 (4)	0.50		
5.0	24(*c*)*				0.20		
	16(*a*)				0.40	(1.00)	(0.00)
	24(*d*)				0.47	(1.00)	(0.00)
	96(*h*)	−0.0274 (5)	0.0546 (5)	0.1493 (6)	0.32		

* Wyckoff notation, 24(*c*), 16(*a*), 24(*d*) and 96(*h*) represent the eight-, six and four-coordinated sites and O atoms, respectively.
† The occupancy parameters for the specimen with the composition $x = 3.8$ were fixed at the values in parentheses.

was performed. After several cycles of refinements, temperature factors were converted to the anisotropic model.

For the composition $x = 3.8$, the occupancy parameter of Ga^{3+} in the four-coordinated site was determined as 1.01 after several cycles of refinements (Table 2). The value shows that all the four-coordinated sites are occupied by Ga^{3+}. Therefore, for this composition, the occupancy parameter of Ga^{3+} in the four-coordinated site was fixed at 1.00. The final R and wR factors for each specimen reached 1.3–2.1% and 1.4–2.2%, respectively (Table 1). The R factors used were

$$R = \Sigma(||F_o| - |F_c||)/\Sigma|F_o|$$

and

$$wR = [\Sigma w(||F_o| - |F_c||)^2/\Sigma w|F_o|^2]^{1/2},$$

with the weighting scheme $w = 1/\sigma^2(F_o)$. For each specimen, $(\Delta\rho)_{max} = 0.7$, 0.6, 0.5, 0.6, 0.6 0.6, 1.0, 0.7, 0.6 and 0.7, and $(\Delta\rho)_{min} = -0.2$, −0.2, −0.1, −0.1 −0.1, −0.1, −0.2, −0.2, −0.1 and −0.2 e Å^{-3} (of the order $x = 0.0$–5.0). The refined positional and occupancy parameters and isotropic equivalent temperature factors are listed in Table 2. The interatomic distances are given in Table 3.*

Results and discussion

Cation distribution

The valence sums around O atoms calculated using the parameters determined empirically by Brown (1981) are 1.97, 1.98, 1.98, 1.98, 1.98, 1.98, 1.98, 1.99, 1.98 and

* Lists of structure factors and anisotropic thermal parameters have been deposited with the IUCr (Reference: OH0041). Copies may be obtained through The Managing Editor, International Union of Crystallography, 5 Abbey Square, Chester CH1 2HU, England.

Table 3. *Interatomic distances* (Å)

(*a*) Cation–oxygen interatomic distances

Composition (x)	d_4	d_6	d_{80}	d_8	d_{8av}
0.0	1.871 (5)	2.015 (5)	2.357 (5)	2.431 (4)	2.394
1.0	1.850 (4)	2.024 (4)	2.357 (4)	2.437 (4)	2.397
1.6	1.841 (6)	2.028 (6)	2.356 (6)	2.438 (6)	2.397
2.0	1.846 (5)	2.023 (5)	2.349 (5)	2.437 (5)	2.393
2.5	1.849 (5)	2.018 (5)	2.344 (5)	2.434 (5)	2.389
3.0	1.844 (5)	2.018 (5)	2.342 (5)	2.431 (5)	2.387
3.6	1.840 (4)	2.011 (4)	2.346 (4)	2.437 (4)	2.392
3.8	1.835 (7)	2.004 (7)	2.345 (7)	2.445 (7)	2.395
4.6	1.845 (5)	1.992 (5)	2.342 (5)	2.439 (5)	2.391
5.0	1.847 (7)	1.980 (7)	2.340 (7)	2.440 (7)	2.390

(*b*) Polyhedral shared edges (Å)

Composition (x)	d_{48}	d_{68}	d_{88}
0.0	2.846 (10)	2.684 (8)	2.784 (9)
1.0	2.817 (9)	2.711 (8)	2.788 (9)
1.6	2.803 (12)	2.723 (10)	2.788 (12)
2.0	2.803 (11)	2.709 (9)	2.782 (10)
2.5	2.805 (10)	2.698 (9)	2.777 (10)
3.0	2.799 (11)	2.700 (9)	2.772 (10)
3.6	2.799 (8)	2.699 (6)	2.792 (7)
3.8	2.792 (14)	2.698 (12)	2.808 (13)
4.6	2.808 (10)	2.674 (8)	2.807 (10)
5.0	2.812 (14)	2.658 (12)	2.816 (13)

(*c*) Polyhedral unshared edges (Å)

Composition (x)	d_{41}	d_{61}	d_{81}
0.0	3.154 (8)	3.006 (8)	2.973 (9)
1.0	3.119 (8)	3.005 (8)	2.964 (9)
1.6	3.103 (10)	3.006 (10)	2.960 (12)
2.0	3.114 (9)	3.004 (9)	2.969 (10)
2.5	3.121 (8)	3.001 (9)	2.974 (9)
3.0	3.112 (9)	3.001 (9)	2.966 (9)
3.6	3.103 (6)	2.982 (7)	2.965 (7)
3.8	3.094 (12)	2.964 (12)	2.971 (13)
4.6	3.110 (8)	2.953 (9)	2.972 (10)
5.0	3.114 (12)	2.934 (12)	2.977 (13)

1.99 for respective compositions (of the order $x = 0.0$–5.0). The values are reasonably acceptable for the site occupancy.

According to the notation proposed by Gilleo & Geller (1959), the chemical formula in the $Y_3Fe_{5-x}Ga_xO_{12}$ system can be generally expressed as

$$\{Y\}_3[Fe_{1-p}Ga_p]_2(Fe_{(3-x+2p)/3}Ga_{(x-2p)/3})_3O_{12},$$

where { }, [ ], ( ), p and x refer to the eight-, six-, and four-coordinated sites, the occupancy parameter of Ga^{3+} in the six-coordinated site and the composition for specimens, respectively. Fig. 2 shows the variations of f_{Ga} and f_{Fe} against the composition x, together with f_{Ga} of Fischer *et al.* (1966), where

$$f_{Ga} = 1 - 2p/x$$

and

$$f_{Fe} = 2(1 - p)/(5 - x).$$

Ga^{3+} and Fe^{3+} are distributed randomly on both the four- and six-coordinated sites when f_{Ga} and f_{Fe} values are 0.6 and 0.4, respectively. This is because the cation ratio between the six-and four-coordinated sites is 2:3. The present result indicates that f_{Ga} values are considerably larger than 0.6, regardless of increasing substitution of Ga^{3+}, for all compositions (Fig. 2*a*). The result is coincident with that of Fischer *et al.* (1966; powder X-ray and neutron diffraction methods). In other words, Ga^{3+} significantly prefers the four-coordinated site. In spite of the larger effective ionic radius of Ga^{3+} compared with that of Al^{3+} (Shannon, 1976), Marezio *et al.* (1968: X-ray single-crystal method) also showed Ga^{3+} preference to the four-coordinated site in $Y_3Al_{5-x}Ga_xO_{12}$. In $Y_3Fe_{5-x}Al_xO_{12}$, Fischer *et al.* (1975) indicated that the smaller Al^{3+} is preferred to the four-coordinated site. Considering the results of the cation site preference for $Y_3Al_{5-x}Ga_xO_{12}$ and $Y_3Fe_{5-x}Al_xO_{12}$, Ga^{3+} preference to the four-coordinated site in $Y_3Al_{5-x}Ga_xO_{12}$ seems to be due to the nature of Ga^{3+} itself and not to Al^{3+} preference for the six-coordinated site. Ions with the d^{10} electron configuration strongly tend to form sp^3-hybrid orbitals. Thus, in $Y_3Fe_{5-x}Ga_xO_{12}$ and $Y_3Al_{5-x}Ga_xO_{12}$ systems, Ga^{3+} preference for the four-coordinated site is probably caused by the strong covalency of Ga^{3+} rather than by the effect of ionic radius.

As shown in Fig. 2, the preference of Ga^{3+} to the four-coordinated site is more evident than stated in Fischer *et al.* (1966). In the composition range $x = 0.0$–1.6 (region I), all Ga^{3+} ions occupy only the four-coordinated site

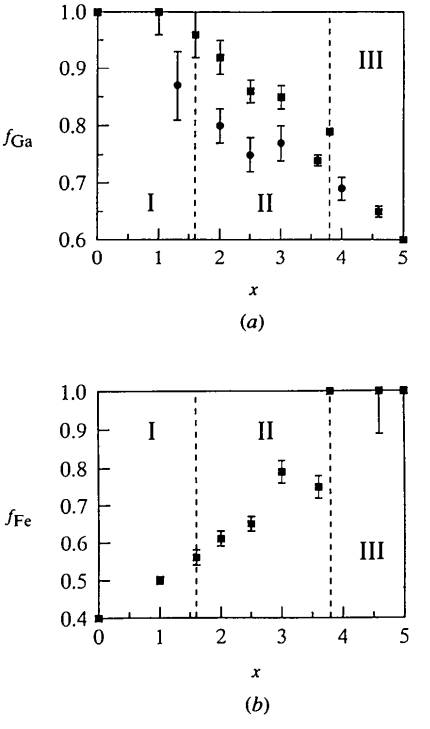

Fig. 2. The variations of the fractional parameters of Ga^{3+} (f_{Ga}) and Fe^{3+} (f_{Fe}) to the four- and six-coordinated sites, respectively. (*a*) and (*b*) show f_{Ga} and f_{Fe} values plotted against composition (x), respectively. The f_{Ga} and f_{Fe} values at both end members ($x = 0.0$ and 5.0) are defined as 1.0, respectively. The cations are distributed randomly when f_{Ga} and f_{Fe} values are 0.6 and 0.4, respectively. Solid square (■), this study; solid circle (●), Fischer *et al.* (1966).

(Fig. 2*a*), whereas Fe^{3+} occupies only the six-coordinated site from $x = 5.0$ to 3.8 (Fig. 2*b*, region III). On the other hand, in the composition range $x = 1.6$–3.8, the two ions occupy both sites (region II). Obviously the tendency for site preferences of Ga^{3+} and Fe^{3+} changes around $x = 1.6$ and 3.8, respectively.

Variation of polyhedra with site preference of cations

Fig. 3 shows the variation of the cation–oxygen distances against the composition. The interatomic distances d_i ($i = 4$, 6, 8, 80, 48, 68, 88, 41, 61, 81, 82 and 83) are labeled in Fig. 1. With increasing Ga^{3+} content in region I and increasing Fe^{3+} content in region III, d_4 decreases whereas d_6 and d_{8av} increase, where d_{8av} is the average of d_{80} and d_8. This indicates the shift of O atoms to the four-coordinated site due to contraction of the tetrahedron and expansion of the octahedron. On the other hand, a reverse tendency is found when the composition changes from regions I or III into II, and O atoms are shifted to the six-coordinated site.

Fig. 4 shows the variation of the difference between the unshared and the shared edges of the polyhedra against the composition, where in the triangular dodecahedron the difference between the shortest (d_{81}) of the three symmetrically nonequivalent unshared edges (d_{81}, d_{82} and d_{83}) and the edge (d_{88}) shared with the other dodecahedron is plotted (Fig. 4*c*). With increasing Ga^{3+} content in region I and increasing Fe^{3+} content in region III, shared edges are lengthening compared with the unshared edges. Around the points where the tendency for site preference of cations is changing ($x = 1.6$ and 3.8), the difference between unshared and shared edges becomes smallest. On the other hand, the shared edges are shortening compared with the unshared edges, when the composition shifts from regions I or III into II.

In silicate garnets, d_{48} is shorter than d_{68} (*e.g.* Euler & Bruce, 1965; Novak & Gibbs, 1971; Meagher, 1975). In

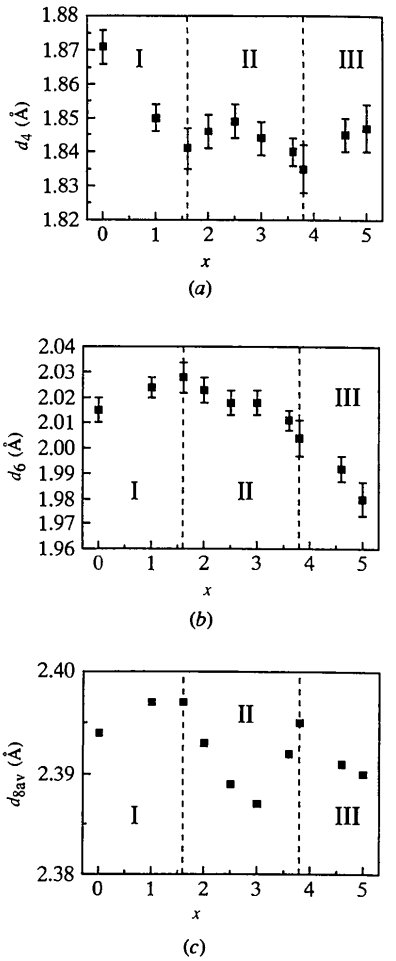

Fig. 3. The mean cation–oxygen interatomic distances plotted against the composition (x). (*a*), (*b*) and (*c*) show the variations of d_4, d_6 and d_{8av} against the composition (x), respectively.

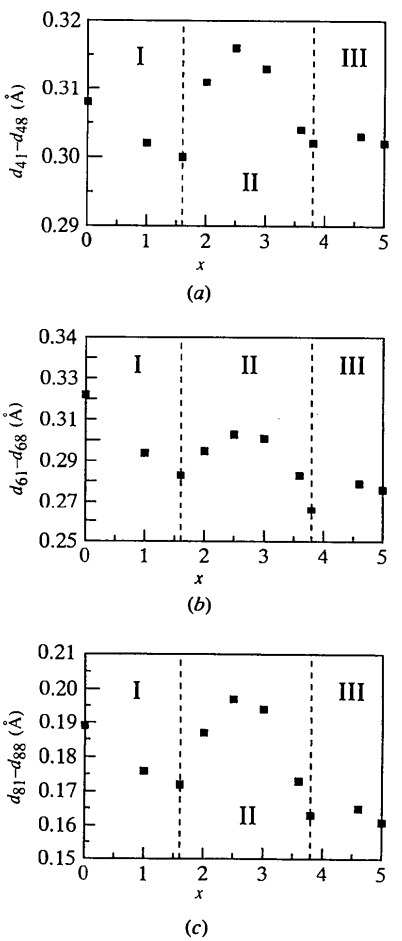

Fig. 4. The difference between the unshared and the shared edge in each polyhedron plotted against composition (x). (*a*), (*b*) and (*c*) show the variations of d_{41}–d_{48}, d_{61}–d_{68} and d_{81}–d_{88} against composition (x), respectively.

$Y_3Fe_{5-x}Ga_xO_{12}$, however, the relation is reversed (Table 3*b*) and d_{48} is longer than in silicate garnets. These facts should be mainly due to the geometric restriction caused by the different cation size in the four-coordinated site. In a simple ionic model, when the shared edge is lengthened by such geometric restriction due to the different cation size, it can be anticipated that the shielding effect of the anions is weakened and the repulsive force between the cations across the shared edges becomes greater. The tetrahedron consists of equivalent two shared edges (d_{48}) and four unshared edges (d_{41}). In Fig. 5 (*ORTEP* plot for YIG; Johnson, 1965), thermal vibrations of both the cations in the four- and the eight-coordinated sites are shown to be significantly smaller in the direction perpendicular to d_{48}, and to be significantly greater in the direction perpendicular to d_{41}. This can be due to the fact that the neighbor atoms for the cation in the four-coordinated site do not exist in the direction perpendicular to d_{41}, whereas the second-neighbor cations (dodecahedral cations) exist in a direction perpendicular to d_{48}. In addition, the thermal vibration of these cations is smaller between both the cations than in the direction of the bonds. These indicate that thermal vibrations are certainly restrained between the cations in the eight- and in the four-coordinated sites. Therefore, we cannot ignore the cation–cation interaction, and it can be presumed that the repulsive force between the cations across d_{48} is large. The relation between the shared and the unshared edges described above (d_{41}–d_{48}, d_{61}–d_{68}, d_{81}–d_{88}) is also caused by the geometric restrictions due to the variation of cation size. It can be anticipated that such geometric restriction with increasing Ga^{3+} content in region I and with increasing Fe^{3+} content in region III yields the decrease of the shielding effect, *i.e.* the enhancement of the repulsive force between the cations across the shared edges. Consequently, the repulsive force between each site across the shared edges will become greatest around the composition $x = 1.6$ and 3.8. On the other hand, when the composition shifts from regions I or III into II, the enhancement of the shielding effect can be anticipated.

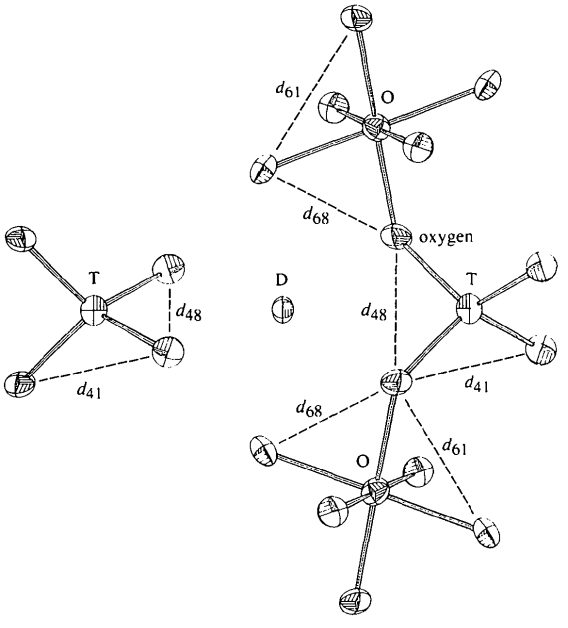

Fig. 5. Thermal motion of Y, Fe and O atoms in the $Y_3Fe_5O_{12}$ garnet structure projected on (010). Atoms are drawn as ellipsoids of 99% probability (*ORTEP*; Johnson, 1965). T, O and D in this figure represent the four-, six- and eight-coordinated sites, respectively.

Ionicity for cation–oxygen bonds

In order to estimate the averaged ionicity of the cation–oxygen bonds, Fig. 6 shows the deviations of d_4, d_6, d_8, d_{80} and d_{8av} from the respective ideal values d_{4ideal}, d_{6ideal} and d_{8ideal}. The ideal values were calculated from the effective ionic radii (Shannon, 1976), based on the results of site occupancy. The ionicity should enhance with increasing cation–oxygen distances because the overlap between orbitals decreases, *i.e.* the increase of d_{8av}–d_{8ideal} and d_6–d_{6ideal} with increasing Ga^{3+} content in region I and with increasing Fe^{3+} content in region III will enhance the ionicity for d_{8av} and d_6 bonds, whereas the decrease in d_4–d_{4ideal} will yield the

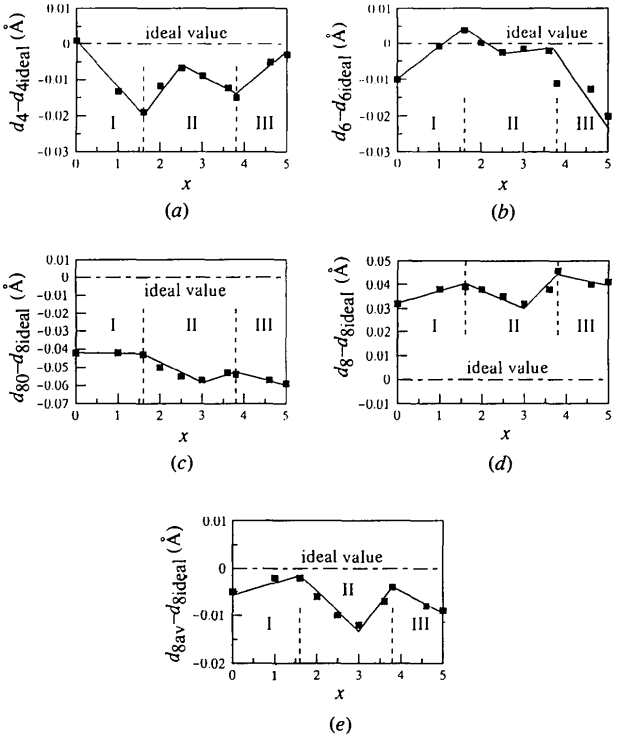

Fig. 6. Deviation of the cation–oxygen distances from respective ideal values plotted against composition (x) in order to estimate ionicity for the cation–oxygen bonds. (*a*), (*b*), (*c*), (*d*) and (*e*) show the variations of d_4–d_{4ideal}, d_6–d_{6ideal}, d_{80}–d_{8ideal}, d_8–d_{8ideal} and d_{8av}–d_{8ideal} against composition (x), respectively.

decrease of the ionicity for the d_4 bond. The reverse tendencies for the ionicity of all cation–oxygen bonds can be observed with the change of tendency for site preference.

The cation–cation interaction should be influenced not only by the decrease of the shielding effect, but also by the enhancement of the ionicity for the cation–oxygen bonds. The variation of the ionicity of the d_4 bond shows the reverse tendency compared with that of d_{8O} and d_6 bonds, whereas that of the d_6 bond shows the same tendency as that of the d_{8av} bond (Fig. 6). Consequently, with increasing Ga^{3+} content in region I and increasing Fe^{3+} content in region III, it can be considered that the cation–cation interaction intensifies between the six- and eight-coordinated sites and between the eight- and the other eight-coordinated sites, whereas it is weakened between the four- and the six-coordinated sites and the four- and the eight-coordinated sites. Thus, the increase of the cation–cation interaction caused by the enhancement of the ionicity will be more significant between the six- and the eight-coordinated sites and between the eight- and the other eight-coordinated sites.

It is interesting that the d_4 bond is close to the ideal ionicity in both end members, whereas the d_6 bond is close in medium compositions (*ca* $x = 2$–4). In addition, the d_{8O} bond shows strong covalency, whereas the d_8 bond has strong ionicity.

Compositional dependence of lattice constants

Fig. 7 shows the variation of the lattice constant (a_0) against composition, showing the deviation from Vegard's law. The lattice constants are greater than those of the ideal values following Vegard's law for the whole composition range. In addition, two nicks can be recognized near $x = 1.6$ and 3.8, supporting the change for site preference of the cations as described above. The variation of the lattice constant in regions I and III is smaller and larger than expected for random distribution of the cations (Vegard's law), respectively. The variation of the lattice constant in region II is larger than in region I, while it is smaller than in region III.

If the cation–cation interaction presumed above exists, the interaction should affect the variation of the lattice constants. This is because the variation of the cation–cation distances directly reflects that of the lattice constants since all cations are located at special positions. In order to presume the lattice constants for silicate garnets from the effective ionic radii, Novak & Gibbs (1971) proposed the following equation

$$a = 9.04\,(2) + 1.61\,(4)\langle r_8\rangle + 1.89\,(8)\langle r_6\rangle. \qquad (1)$$

In our study, (1) cannot be applied directly because the cation size in the four-coordinated site varies. Hence, in order to account for the variation of cation size in the four-coordinated site, we defined the following equation

$$a_0 = 1.61\langle r_8\rangle + 1.89\langle r_6\rangle + \alpha\langle r_4\rangle, \qquad (2)$$

where $\langle r_8\rangle$, $\langle r_6\rangle$ and $\langle r_4\rangle$ are the mean cation size in the eight-, six- and four-coordinated sites, respectively, a, a_0 and α are the presumed lattice constants of silicate garnets, the measured lattice constants in this study and the coefficient of $\langle r_4\rangle$, respectively. If the variation of the lattice constants seen in Fig. 7 is yielded only by the variation of cation size, the α values for the whole composition range should be constant since the value of 9.04 in (1) corresponds to $\alpha\langle r_4\rangle$ in (2) and depends only on the cation size in the four-coordinated site (Si^{4+}). As seen in Fig. 8, the α values are not constant and increase greatly with increasing Ga^{3+} content. Consequently, it can be said that the variation of the lattice constants cannot be explained only by the effect of cation size and is closely related to the cation–cation interaction.

The effect of the cation–cation interaction on the variation of the lattice constants can be explained as follows. With increasing Ga^{3+} content in region I and increasing Fe^{3+} content in region III, the shortening of

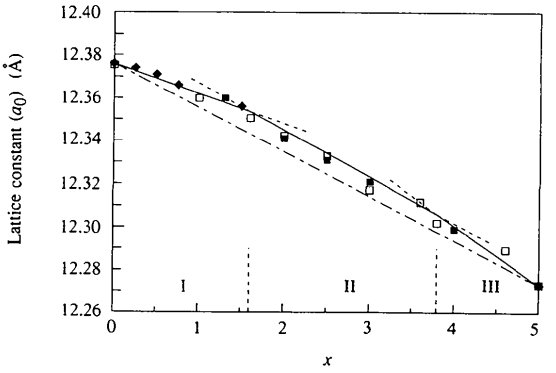

Fig. 7. Variation of lattice constants (a_0) against composition (x). — · — shows ideal variation following Vegard's law. Open square (□), this study; solid square (■), Fischer *et al.* (1966); solid diamond (◆), Gilleo & Geller (1958).

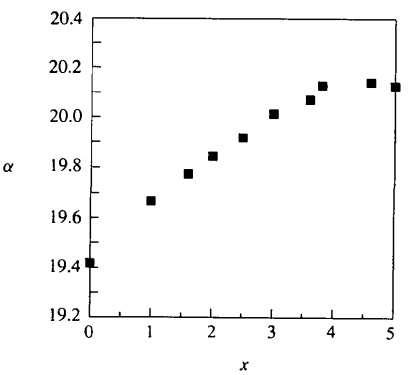

Fig. 8. The coefficient α defined by the present study, $a_0 = 1.61\langle r_8\rangle + 1.89\langle r_6\rangle + \alpha\langle r_4\rangle$, is plotted against composition (x). When α values are constant, the variation of the lattice constants (a_0) depends only on cation size of the respective sites.

the cation–cation distances is avoided as far as possible in order to keep the cation–cation interaction to a minimum. On the other hand, when the composition shifts from regions I or III into II, the shortening is accepted because of the relaxation of the cation–cation interaction.

The interpretation of site preference

The causes for the change in tendency for site preference will be due to some structural or energetic instability around the changing points, $x = 1.6$ and 3.8. In silicate garnets, Novak & Gibbs (1971) introduced the stable region from the effective ionic radii of cations in the eight- and six-coordinated sites. If such a stable region also exists for garnets with trivalent cations, the two significant factors for structural stability are first-neighbor cation–anion and anion–anion distances. As seen in Fig. 6, d_6 and d_{8av}, at $x = 1.6$ and 3.8, are close to the expected distances (ideal values) and are reasonable; d_4 at $x = 1.6$ and 3.8 are 0.019 and 0.015 Å shorter than the ideal value, respectively. These values, however, are not small enough to be anomalous for structural stability. In addition, all O—O distances are reasonable, and no O—O distances are short enough to introduce the strong repulsive force between oxygens (Tables 3*b* and *c*). Consequently, in the above two factors for structural stability, the anomalies cannot be found at $x = 1.6$ and 3.8.

Cation–cation interactions can be considered as the other factor of instability. As described above, the geometric restrictions set from the concentration of the smaller Ga^{3+} in only the four-coordinated site and the larger Fe^{3+} in only the six-coordinated site will force an increase in the cation–cation interaction by decreasing the shielding effect and increasing the ionicity for d_6 and d_{8av} bonds. The increase of the interaction should enhance the energetic instability. In order to relax the energetic instability, the increased shielding effect and the decreased ionicity for d_6 and d_{8av} bonds are indispensable, *i.e.* the relative shortening of the polyhedral shared edges and of d_6 and d_{8av} are necessary. As described above, such relative shortening is brought about by the change in tendency for site preference of cations. Consequently, it can be considered that the change in tendency is caused in order to relax the increased cation–cation interaction. The compositions around $x = 1.6$ and 3.8 are probably acceptable limits for the repulsive force caused by the cation–cation interaction.

As evident from Fig. 5, it can be considered that the effect of the cation–cation interaction on the change in tendency for site preference of cations is greatest between the four- and the eight-coordinated sites, when we consider the thermal ellipsoids. However, the increase in interactions between the four- and eight-coordinated sites and between the four- and six-coordinated sites is probably only due to the effect caused by the decrease of the shielding effect, whereas that between the six-and eight-coordinated sites and between the eight- and the other eight-coordinated sites is probably caused by both the decrease of the shielding effect and the increase of the ionicity for d_6 and d_{8av} bonds. Moreover, the cation–cation distance between the six- and the eight-coordinated sites is shorter than that between the eight- and the other eight-coordinated sites. Consequently, the cation–cation interaction between the six- and the eight-coordinated sites will also contribute somewhat to the change in tendency for site preference, together with that between the four- and the eight- coordinated sites.

The authors wish to thank Professor Dr F. Kanamaru of Osaka University, Dr R. Kitagawa of Hiroshima University for most valuable discussions, Dr M. Setoguchi of Government Industrial Research Institute, Osaka, for advice in the synthesis experiment and Mr T. Tanaka of Osaka University for help in the operation of the X-ray equipment. Thanks are also due to Mr A. Minami of Hiroshima University for the chemical analysis by XMA. Intensity measurements were performed at The Materials Analyzing Center, The Institute of Scientific and Industrial Research, Osaka University.

References

BERTAUT, F. & FORRAT, F. (1956). *C. R. Acad. Sci. Paris*, **242**, 382–384.

BONNET, M., DELAPALME, A., FUESS, H. & THOMAS, M. (1975). *Acta Cryst.* B**31**, 2233–2240.

BROWN, I. D. (1981). *Structure and Bonding in Crystals*, edited by M. O'KEEFFE & A. NAVROTSKY, Vol. II, pp. 1–30. New York: Academic Press.

CHENAVAS, J., JOUBERT, J. C., MAREZIO, M. & FERRAND, B. (1978). *J. Less-Common Met.* **62**, 373–380.

EULER, F. & BRUCE, J. A. (1965). *Acta Cryst.* **19**, 971–978.

FINGER, L. W. (1969). Determination of cation distribution by least-squares refinement of single-crystal X-ray data. *Carnegie Inst. Washington Yearb.* **67**, 216–217.

FISCHER, P., HÄLG, W., ROGGWILLER, P. & CZERLINSKY, E. R. (1975). *Solid State Commun.* **16**, 987–992.

FISCHER, P., HÄLG, W., STOLL, E. & SEGMÜLLER, A. (1966). *Acta Cryst.* **21**, 765–769.

GELLER, S. & GILLEO, M. A. (1957). *Acta Cryst.* **10**, 239.

GILLEO, M. A. & GELLER, S. (1958). *Phys. Rev.* **110**, 73–78.

GILLEO, M. A. & GELLER, S. (1959). *J. Phys. Chem. Solids*, **10**, 187–190.

GUILLOT, M., LE GALL, H. & LEBLANC, M. (1990). *J. Magn. Magn. Mater.* **86**, 13–18.

JOHNSON, C. K. (1965). *ORTEP*. Report ORNL-3794. Oak Ridge National Laboratory, Tennessee, USA.

MAREZIO, M., REMEIKA, J. P. & DERNIER, P. D. (1968). *Acta Cryst.* B**24**, 1670–1674.

MEAGHER, E. P. (1975). *Am. Mineral.* **60**, 218–228.

MENZER, G. (1926). *Z. Kristallogr.* **63**, 157–158.

NOVAK, G. A. & GIBBS, G. V. (1971). *Am. Mineral.* **56**, 791–825.

POPMA, T. J. A., VAN DIEPEN, A. M. & ROBERTSON, J. M. (1974). *Mater. Res. Bull.* **9**, 699–704.

SHANNON, R. D. (1976). *Acta Cryst.* A**32**, 751–767.